Estimation of long-wavelength near-surface velocity and low-relief structural anomalies Part I. A case history in central Saudi Arabia

Peter I. Pecholcs and Sun Nguyen, Saudi Aramco; Dan Kosloff and Alex Litvin, Paradigm Geophysical*

Summary

Undetected near-surface and subsurface velocity variations greater than an effective spread length produce false structures both in time and depth. The estimation of these variations rely on uphole measurements, high density shallow reflection data and sufficiently long offsets for subsurface reflectors. Despite inadequate near-surface velocity-depth measurements in the study area, we developed a strategy for the detection and estimation of both near-surface and subsurface long-wavelength velocity and low-relief structural variations. We chose two 2D seismic lines (dip and strike) over two existing low-relief fields in central Saudi Arabia, to demonstrate how the velocity-depth ambiguity problem is partially overcome by integrating the refraction delay time solutions derived from multiple refractors below the seismic reference datum with iterative pre-stack depth migration, residual analysis, and reflection tomography. We compare these results with the conventional isopach depthing method and discuss how this strategy improves the structural integrity of potential prospects. Even with the verification of the near-surface velocity and structural anomalies along the dip line and buried velocity anomaly along the strike line through forward modeling and flatness of depth image gathers, these models are non-unique. Based upon this case study, a new constrained tomographic algorithm has been developed which overcomes the above ambiguity and is discussed in Part II.

Introduction

In central Saudi Arabia, 2D seismic data is acquired along lines (greater than 70 km) over near-surface conditions which include different combinations of sand lenses, buried channels, leaching, outcropping formations, and in some areas the effects of a shallow unconfined aquifer. These variable near-surface conditions give rise to lateral velocity variations and thus to time anomalies of wavelengths of different scales, from as small as a cdp interval to much greater than a cable length. The base of weathering for short wavelength velocity variations is confined to several tens of meters below the surface and extends well below the seismic reference datum (SRD) for long wavelength lateral velocity variations. In the study area, the sparsely spaced and shallow uphole control points could not be used to generate a reliable 3D average velocity model because the base of weathering is well below the maximum uphole penetration depth and SRD. Fortunately, the spatially varying unconsolidated sand is underlain by deeper multiple refractors. The refracted arrival times from these horizons can be reliably picked and a delay time solution calculated. But without accurate velocity or depth of weathering control, a velocity-depth ambiguity problem exists and a unique refraction static solution cannot be obtained from accurate delay times (Archer and Heathcote, 1985). With the cessation of the uphole program, we rely on the creative interpretation skill of the interpreter and the near-surface modeler. The interpreted near-surface velocity-depth model is used to calculate and apply datum statics to the stacked time section which effectively shifts the zero-offset sources and receivers to the SRD. This datum corrected stacked time section is assumed to be free of all near-surface lateral velocity-depth variations. If this assumption is correct and the subsurface velocities are relatively constant the time section will be conformable with the depth section.

Prospect generation begins by identifying time anomalies, interpreting time horizons, and converting these time horizons to depth horizons. The process of converting a time section to a depth section ultimately determines if these time anomalies have any commercial value. There are several top-down approaches available for converting a time section to a depth section and all depend on the initial near-surface velocity-depth model. Recent field work has shown the existence of significant post-Triassic surface folds. Two opposing theories suggest they were formed by anhydrite dissolution and collapse or basement reactivation. In the first case, the velocity/depth anomaly is independent of the initial basement generated subsurface structure. and a simple bulk shift of the isopach model could correct the depth error during drilling analysis. In the second case, the near-surface structure formed during basement reactivation. Therefore, misinterpretation of the near-surface velocity/depth model will affect the vertical and lateral extent of the deeper Triassic structure.

The purpose of this paper is to show how to improve the structural integrity of potential prospects with similar near-surface conditions. A strike and dip line were selected over two existing low-relief fields which cover an area with nearly flat surface topography and formations dipping at angles less than one degree. We discuss how independent near-surface velocity-depth models constructed from upholes and refraction delay time

solutions can affect the conventional isochron/isopach depthing procedure. Finally, we develop a strategy for integrating refraction static near-surface depth models with a pre-stack depth migration and constrained reflection tomography strategy to improve the accuracy of both the near-surface and deeper velocity-depth section.

Geologic setting and acquisition

The low-relief prospects are situated in central Saudi Arabia which is characterized by formations dipping less than one degree to the north-east. Shallow lateral velocity variations are caused by unconsolidated sands which are underlain by an unconfined aquifer above an anhydrite layer which extends down to approximately 600 meters, and outcropping formations. These unconsolidated sands introduce short wavelength time shifts which affect the stacking power, while the combination of laterally outcropping formations and water-saturated sands introduce a long wavelength time shift. These unconsolidated sands overly the consolidated Cretaceous sand (H02) which overlies the Upper Jurassic anhydrite (H03). The measurable impedance contrasts at the top of the water table (H01), top of H02, and HO3 generate observable refracted head waves. These head waves are interpreted as third (A), second (B), and first break (C) arrival times, respectively, on the shot records (Fig. 1). The average velocities for layer above H01, H02, and H03 are approximately 2000 m/s, 2200 m/s, and 3800 m/s, respectively. The average velocity of anhydrite is 5000 m/s.

The seismic survey recorded 480 channel split-spread (240 fold - 12.5 meter CMP interval) along eleven dip lines (West-East) and a single strike line (North-South). The vibrator sweep frequency was 8 to 64 hertz and 14000 ms in length. Initial structural mapping of the target horizon produced two prospects. Prospect A measures approximately six kilometers along the dip line and twelve kilometers along the strike line. and prospect B measures approximately six kilometers along the strike line and three kilometers along the dip line. Two discovery wells (A1 and M1) were drilled along the strike line and a third delineation well (A2) was drilled along the dip line.

Time processing and near-surface velocity-depth model construction

During 1993-1996, three different time processing flows were applied to the study area for the purpose of improving the reflector continuity within the target zone, constructing an accurate near-surface velocity-depth datum statics model, and to better understand how these models affect the geometry of deeper low relief time and depth structures.

The initial processing sequence applied to the data was: field statics from the uphole near-surface model, first pass residual from non-fk data, fk filter on shot records, automatic gain control, surface-consistent deconvolution, velocity analysis, residual statics, radon multiple elimination, velocity analysis, normal moveout correction, mute, time-variant filter, CMP stack, 4:1 sum, gain, and datum corrected to SRD. The initial interpretation based upon isochron thinning provides the basis for establishing structural deformation during the Triassic. However, the generation of time maps are limited by the uphole datum static model. The oversimplification of the near-surface long-wavelength velocity variation may not change the overall position of the structural high but will distort the size and shape. The refraction statics method can help resolve these apparent long wavelength time structures.

In the second approach, conventional refraction delay times and refractor velocities were calculated (Taner T. et al., 1992) using the first break traveltimes (C) from horizon (H03) and the near-surface depth model was constructed from delay times using a constant overburden velocity. The refraction statics correction is accomplished in two steps. In the first step, the correction from surface to the refractor uses the overburden velocity and in the second step the correction uses a replacement velocity of 4800 m/s from refractor to SRD. These results mistied the uphole datum static solution from the first approach by as much as 200 ms along the dip line (Fig. 2).

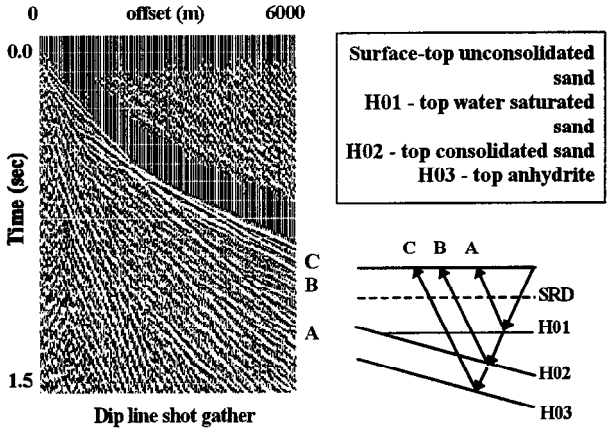

Figure 1: Shot gather display (Shot point 3500) Refracted arrivals from H01, H02, and H03 can be identified as the third (A), second (B), and first (C) break arrival times.

These differences are caused by different overburden velocities and base of weathering depths. Both approaches removed the effects of topography and laterally varying velocity in between the surface and SRD however the second approach also removed the velocity-depth variation from SRD to HO3 and replaced this wedge with a constant velocity of 4800 m/s. The two resulting time sections are

both referenced from SRD but display different apparent time dips due to two different datum static corrections..-

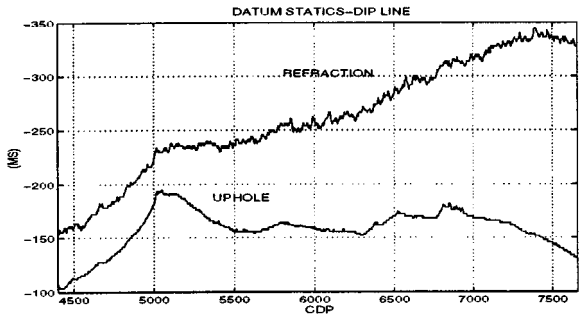

Figure 2. Uphole and refractions datum statics for the dip line. Note the 200 ms difference at CMP 7000.

Given this discrepancy in time, a more detailed analysis of the near-surface above H03 is required to resolve this ambiguity. The fmal reprocessing objective was to maximize both the lateral and vertical resolution in the shallow time section. Processing parameters were specially designed and applied to the shallow time section, improving the reflector continuity of the water table (H01) and the shallow refractor (H02). Independent delay time solutions for H02 and H03 were derived from refraction second break picks (B) and first break picks (C) using the same offset range (Fig. 3A). With approximately 40 ms (plus or minus 4 ms) separating the two horizons (Fig. 3B) we assume the velocity and thickness is relatively constant. Hence, H02 is redefmed as the base of weathering.

Using intersecting well control for both the dip and strike lines, a constant velocity was used to build a smooth refractor depth horizon. The resulting depth horizon along the dip line exhibits an apparent low-relief structure overlying the deeper structural deformation.

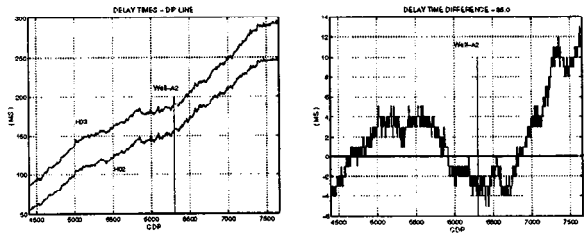

Figure 3. A) Independent delay time solutions for H02 and H03 along the dip line. B) The difference in delay times minus 35 ms.

These near-surface velocity-depth models will introduce errors into the final depth map by the amount of error in the shallow geologic structure and interval velocity assumption. We must be careful not to rely too heavily on datum corrected time sections without accurate overburden velocities.

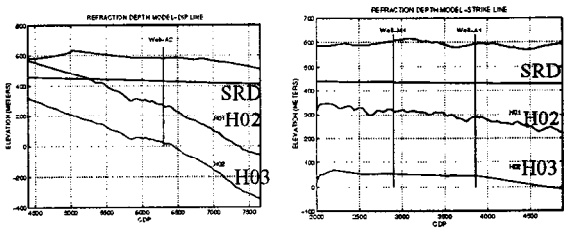

Figure 4. A) Dip line refraction statics near-surface depth model B) Strike line refraction statics near-surface depth model.

Depth processing

As described earlier in this paper, refraction near-surface model construction is non-unique without an accurate overburden velocity or thickness. We have developed a strategy for verification and integration of these models into the time-to-depth conversion process. This was accomplished through synthetic modeling studies with iterative pre-stack depth migration and constrained reflection tomography.

In this study area, we assume the subsurface reflector geometry varies laterally and the interval velocity remains relatively constant while in the near-surface we allow velocity, or thickness, or both to vary. We refer to these three models as model A, B, and C corresponding to the near-surface structural, velocity, and coupled structural/velocity anomalies, respectively. These models assume a flat topography and use the same subsurface isopachs. We preserve the shallow time anomalies in all three cases by using the zero-offset times as the starting model.

Model A uses the near-surface depth horizons HO2 and H03 from the refraction statics model in figure 4A, and assumes a constant overburden velocity of 2000 m/s. The interval velocities for the four subsurface layers below H02 are 3800 m/s (H03), 5000 m/s, 4500 m/s, and 4000 m/s, respectively. Model B removes the structural anomaly in model A by flattening the dipping horizon (H02) and introduces a high velocity lens above it. Model C includes both a laterally varying-velocity and structural anomaly. In all three cases we generated synthetic pre-stack ray trace CMP gathers and a zero-offset time section.

We begin all three tests by pre-stack depth migrating with the same incorrect input velocity-depth model. This model is similar to model A but without the structural anomaly o the first dipping horizon (H02). The subsurface layers are constructed with the same isopachs as above.

We found that in the first case: we could recover the original near-surface structure simply by pre-stack depth migrating and reinterpreting the depth image. The second test successfully used the constrained reflection

tomography algorithm developed by Kosloff et. al., 1996, to reconstruct the near-surface velocity anomaly by constraining the subsurface thicknesses and inputing the subsurface image gather depth delays. In the third case, we could not successfully reconstruct the near-surface velocity and structural anomaly.

In the real data case, we used the refraction statics models in figure 4A and 4B as our starting models. After running pre-stack depth migration, depth delay panels were used to detect and update velocity anomalies in the near-surface layer (dip line) and a subsurface layer (strike line). In the inversion, the thickness of the near-surface layer was kept fixed. The final focused time sections and depth migrated images for the dip and strike lines are shown in figures 5 and 6, respectively. Both cases tie the well data. Forward modeling and flattness of image gathers were used for final model verification.

Conclusions

Careful reprocessing of shallow reflectors and refractors integrated with depth image processing methods can partially remove the velocity-depth ambiguity. The synthetic test cases demonstrate how properly constrained depth imaging problems overcome the velocity-depth ambiguity while the results from the unconstrained inversion must be cautiously interpreted. The fmal depth migrated sections are consistent with apriori geologic and well information.

Acknowledgments

We would like to thank Saudi Aramco's management and especially M. Abdul Baqi for allowing us to publish this paper.

References

Archer, S.H., and Heathcote, C., Can refraction arrival times be used to solve the long wavelength statics problem ?, In *Expanded Abstracts of the 55th Annual International SE G Meeting*, SEG, Houston,1985

Kosloff, D., Sherwood, J., Karen, Z., Machet, E., and Falkovitz,Y. 1996, Velocity and interface depth determination by tomography of depth migrated gathers, Geophysics, 61,1511-1523.

Taner, M. T., Lu, L., and Baysal, E., Unified method for 2-D and 3-D refraction statics with first break picking by supervised learning: *In Expanded Abstracts of the 62nd Annual International SEG Meeting SEG, New* Orleans,1992.

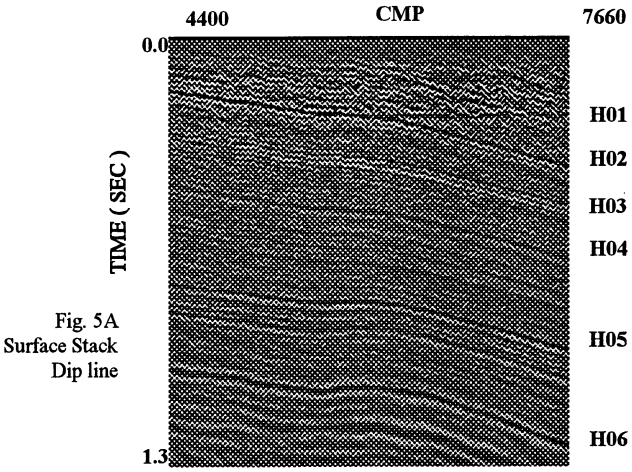

Fig. 5A
Surface Stack
Dip line

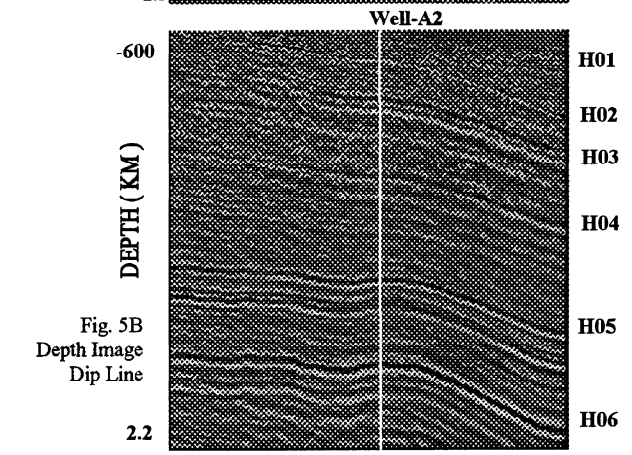

Fig. 5B
Depth Image
Dip Line

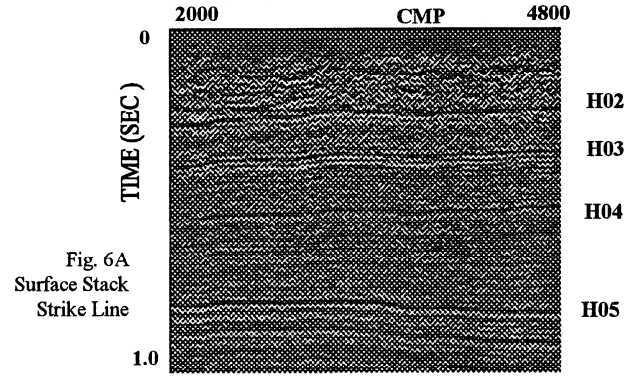

Fig. 6A
Surface Stack
Strike Line

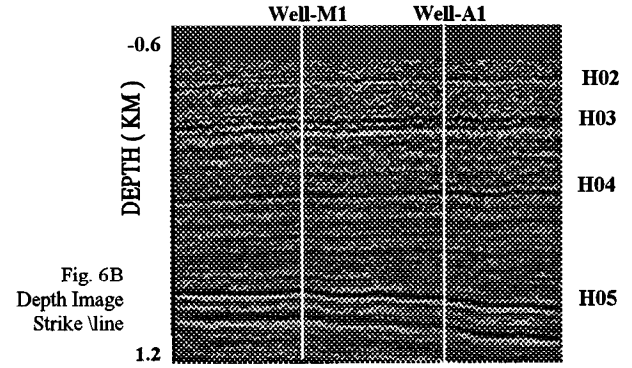

Fig. 6B
Depth Image
Strike \line